Avalanches, breathers, and flow reversal in a continuous Lorenz-96 model

R. Blender, J. Wouters, and V. Lucarini
Meteorologisches Institut, KlimaCampus, Universität Hamburg, Hamburg, Germany
(Received 25 February 2013; published 8 July 2013)

For the discrete model suggested by Lorenz in 1996, a one-dimensional long-wave approximation with nonlinear excitation and diffusion is derived. The model is energy conserving but non-Hamiltonian. In a low-order truncation, weak external forcing of the zonal mean flow induces avalanchelike breather solutions which cause reversal of the mean flow by a wave-mean flow interaction. The mechanism is an outburst-recharge process similar to avalanches in a sandpile model.

DOI: 10.1103/PhysRevE.88.013201 PACS number(s): 05.45.Yv, 47.20.−k, 47.10.Df, 47.35.Bb

I. INTRODUCTION

In 1996 Lorenz suggested a nonlinear chaotic model for an unspecified observable with next- and second-nearest-neighbor couplings on grid points along a latitude circle [1]. Due to its scalability, the model is a versatile tool in statistical mechanics [2–5] and meteorology [6–8]. The nonlinear terms have a quadratic conservation law and satisfy Liouville's theorem. For strong forcing the model shows intermittency [9].

The Lorenz-96 equations for the variable X_i are a surrogate for nonlinear advection in a periodic domain

$$\frac{d}{dt}X_i = X_{i-1}[X_{i+1} - X_{i-2}] - \gamma X_i + F_i, \tag{1}$$

where γ characterizes linear friction ($\gamma = 1$ in [1]) and F is a forcing.

In this paper a continuous long-wave approximation of the Lorenz-96 model is derived. A surprising finding is that the nonlinear terms in the Taylor expansion are associated with a sequence of similar antisymmetric dynamic operators. Furthermore, the dynamics in a truncated version reveals avalanches, breatherlike excitations, and flow reversals which mimic various physical processes in complex systems in a simplistic way.

Lorenz [10] has analyzed the linear stability of the mean m of X_i in (1) and found that long waves with wave numbers $k < 2\pi/3$ are unstable for a positive mean m.

II. LONG-WAVE APPROXIMATION

A continuous approximation is derived for a smooth dependency of X_i on the spatial coordinate $x = ih$ in the limit $h \to 0$. The variable X_i is replaced by a continuous function $u(x,t)$, which is interpreted as velocity. In the following the equations for $\gamma = 0$ are considered.

The expansion of the nonlinear terms in (1) up to order $O(h^2)$ yields, for the rescaled coordinate $x' = -x/3h$ (the prime is dropped below),

$$u_t = -uu_x - \tfrac{1}{3}\left(u_x^2 + \tfrac{1}{2}uu_{xx}\right) + f, \tag{2}$$

with an advection and further nonlinear terms which are due to the noncentered definition of the interaction in (1). For an algebraic derivation of a hierarchy of additional continuous equations, see the Appendix.

The total energy for the velocity $u(x,t)$ is

$$\mathcal{H} = \frac{1}{2}\int u^2 dx, \tag{3}$$

which is conserved for $f = 0$.

The nonlinear terms are associated with the following antisymmetric evolution operators:

$$O(h): \mathcal{J}_1 = -\tfrac{1}{3}(u\partial_x + \partial_x u), \tag{4}$$

$$O(h^2): \mathcal{J}_2 = -\tfrac{1}{6}(u_x\partial_x + \partial_x u_x). \tag{5}$$

Thus the evolution equation (2) can be written as

$$u_t = \mathcal{J}\frac{\delta\mathcal{H}}{\delta u}, \quad \mathcal{J} = \mathcal{J}_1 + \mathcal{J}_2, \tag{6}$$

with the functional derivative $\delta/\delta u$ with respect to u. Note that the $O(h^3)$ expansion in (2) is represented by a third operator $\mathcal{J}_3 = -(1/18)(u_{xx}\partial_x + \partial_x u_{xx})$; here we are restricted to the $O(h^2)$ expansion (2).

The evolution equation (2) has a conservation law for $f = 0$:

$$\partial_t\left(\tfrac{1}{2}u^2\right) = \partial_x\phi, \tag{7}$$

$$\phi = -\tfrac{1}{3}u^3 - \tfrac{1}{6}u^2u_x, \tag{8}$$

with the conserved current ϕ, which leads to the conservation of total energy (3). Further conservation laws could not be found. In particular, momentum given as the mean flow

$$U = \langle u\rangle = \int u dx \tag{9}$$

is not constant.

In the following we consider a constant and positive forcing f (note that the system is not dissipative). In the presence of perturbations v to the mean flow, $u = U + v$, the mean flow energy $\bar{H} = U^2/2$ changes according to

$$\frac{\partial}{\partial t}\bar{H} = -\frac{U}{6}\langle v_x^2\rangle + Uf. \tag{10}$$

The perturbation energy,

$$E' = \tfrac{1}{2}\langle v^2\rangle, \tag{11}$$

grows for positive U,

$$\frac{\partial}{\partial t}E' = \frac{U}{6}\langle v_x^2\rangle. \tag{12}$$

Thus mean flows with $U > 0$ ($U < 0$) are unstable (stable) as in the discrete system (1) analyzed in Ref. [10].

Equations (10) and (12) represent a coupling between perturbations and the mean flow. A forcing drives the mean flow towards positive values, which allow the growth of perturbations. When the perturbation gradients are sufficiently intense, they reduce the flow to negative values, causing a decay of their intensities.

III. LOW-ORDER MODEL

The nonlinear energy cycle represented by the exchange between zonal flow and wave energy in (10) and (12) is analyzed in a spectral model for the unstable long waves by Fourier expansion in a periodic domain $[-\pi,\pi]$:

$$u = \sum_{n=0}^{N} a_n \sin(nx) + b_n \cos(nx). \tag{13}$$

Here we are restricted to the low-order system $N = 2$:

$$\dot{b}_0 = -\tfrac{1}{12}\left(a_1^2 + b_1^2\right) - \tfrac{1}{3}\left(a_2^2 + b_2^2\right) + f, \tag{14}$$

$$\dot{a}_1 = b_0 b_1 + \tfrac{1}{6} b_0 a_1 + \tfrac{1}{2}(a_1 a_2 + b_1 b_2) + \tfrac{1}{4}(a_1 b_2 - b_1 a_2), \tag{15}$$

$$\dot{b}_1 = -b_0 a_1 + \tfrac{1}{6} b_0 b_1 - \tfrac{1}{4}(a_1 a_2 + b_1 b_2) + \tfrac{1}{2}(a_1 b_2 - b_1 a_2), \tag{16}$$

$$\dot{a}_2 = 2 b_0 b_2 + \tfrac{2}{3} b_0 a_2 + \tfrac{1}{2}\left(b_1^2 + a_1 b_1 - a_1^2\right), \tag{17}$$

$$\dot{b}_2 = -2 b_0 a_2 - a_1 b_1 + \tfrac{1}{4}\left(b_1^2 - a_1^2\right) + \tfrac{2}{3} b_0 b_2. \tag{18}$$

The mean flow is $U = b_0$, which is subject to a constant forcing f in the numerical experiments (14). The truncated system conserves energy for $f = 0$ as follows:

$$H_{\mathrm{tot}} = H_0 + H_1 + H_2, \tag{19}$$

$$H_0 = \tfrac{1}{2} b_0^2, \quad H_1 = \tfrac{1}{4}\left(a_1^2 + b_1^2\right), \quad H_2 = \tfrac{1}{4}\left(a_2^2 + b_2^2\right). \tag{20}$$

The Liouville theorem is not satisfied:

$$\sum_{n=0}^{2}\left(\frac{\partial \dot{a}_n}{\partial a_n} + \frac{\partial \dot{b}_n}{\partial b_n}\right) = \tfrac{5}{3} b_0. \tag{21}$$

The expansion and contraction of the state space volume is controlled by the sign of the mean flow.

For $N = 1$ the equations (14)–(16) possess a constant of motion for finite forcing f (see Fig. 1 for $f = 0.1$):

$$H_f = H_0 + H_1 - 3f \log H_1, \tag{22}$$

which reduces to the total energy for $f = 0$. A corresponding conservation law including the $N = 2$ modes could not be found.

IV. FORCED EXPERIMENTS

Numerical experiments are performed for different forcings and truncations (all use the identical initial conditions $b_0 = 1.13, a_1 = 3.4, b_1 = 6.8$, and for $N = 2$: $a_2 = 11, b_2 = 17$).

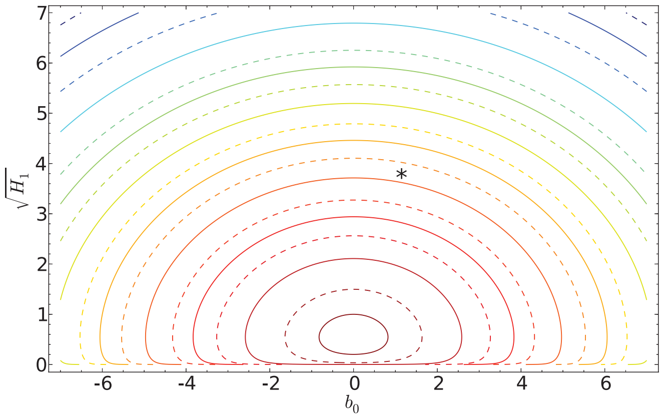

FIG. 1. (Color online) Contour plot of the constant of motion H_f in Eq. (22) for the forcing $f = 0.1$. The asterisk (*) shows the initial condition chosen in the numerical experiments.

(i) Weak forcing with $f = 0.1$ in the $N = 1$ truncation reveals periodic flow reversals (Fig. 2). A mean flow increases gradually to positive values, where it becomes unstable due to the excited waves, denoted as breathers in the following. These breathers drive a rapid flow reversal towards a negative flow which initiates their collapse. Dynamics proceeds counterclockwise along the conservation law $H_f = \mathrm{const}$ (Fig. 1). The avalanche process is most distinct for initial conditions reaching regimes with small wave energy. The process is energy conserving ($H_{\mathrm{tot}} = \mathrm{const}$) on short time scales. The total energy increases (decreases) when the mean flow is positive (negative).

For $N = 1$ with the amplitudes b_0, a_1, b_1, the energy cycle is for $f = 0$ [compare (10), (12)]:

$$\partial_t H_0 = -\tfrac{1}{3} b_0 H_1, \quad \partial_t H_1 = \tfrac{1}{3} b_0 H_1, \tag{23}$$

which is controlled by the mean flow. The solution for the mean flow is for $b_0(0) = 0$,

$$b_0 = -6a \tanh(at), \tag{24}$$

and the perturbation energy is

$$H_1 = \frac{18a^2}{\cosh^2(at)}, \tag{25}$$

where a is related to the total energy $H = 18a^2$. H_1 attains its maximum during flow reversals when $U = 0$. These approximations are compared to the forced simulation in Figs. 2(b) and 2(c), centered at a single flow reversal.

In the presence of forcing f and for a small wave energy H_1, the mean flow b_0 grows linearly in time, $b_0(t) \approx ft$, up to a value $b_{0,\max}$. This defines an interarrival time scale of flow reversals, $\tau = 2b_{0,\max}/f$. In this range the wave energy evolves rapidly according to $H_1(t) \sim \exp(ft^2/6)$.

The described flow reversal mechanism is retained for viscous dissipation represented by a linear damping of the wave amplitudes a_1 and b_1.

For the $N = 2$ truncation with all modes b_0, a_1, b_1, a_2, and b_2, flow reversals occur on a time scale roughly twice as for $N = 1$ [Fig. 2(d)]. Due to the weak forcing the energy cascades to mode 2 with negligible amplitudes a_1, b_1 and energy H_1 [Figs. 2(d) and 2(e)]. Neglecting the modes 1, the energy cycle

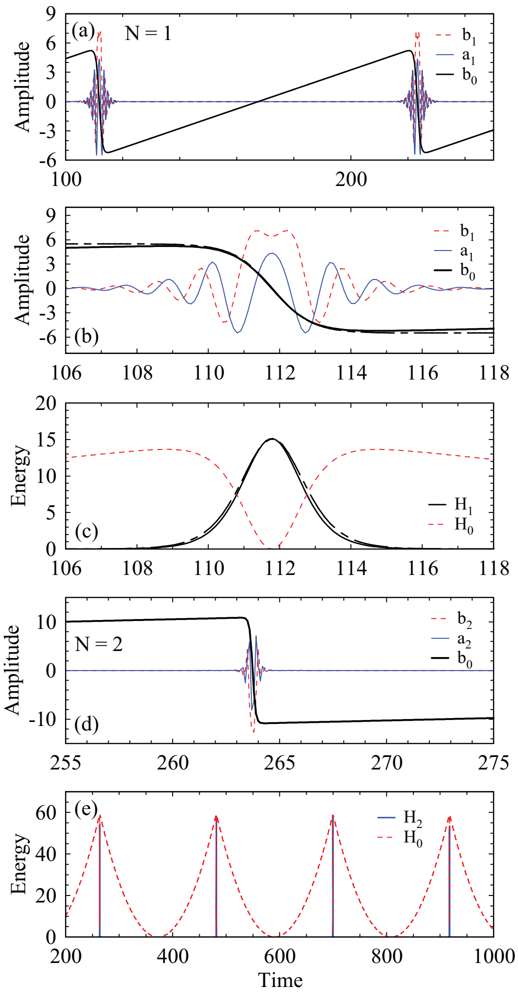

FIG. 2. (Color online) Weak forcing $f = 0.1$: (a) amplitudes b_0,a_1,b_1 for $N = 1$, intervals ≈ 110, (b) amplitudes during a flow reversal with Eq. (24) for b_0 (dashed), (c) energies H_0, H_1 and Eq. (25) for H_1 (dashed), (d) amplitudes b_0,a_2,b_2 for $N = 2$, (a_1,b_1 vanish), and (e) energies (H_1 vanishes).

for interactions among b_0,a_2, and b_2 is

$$\partial_t H_0 = -\tfrac{4}{3} b_0 H_2, \quad \partial_t H_2 = \tfrac{4}{3} b_0 H_2. \tag{26}$$

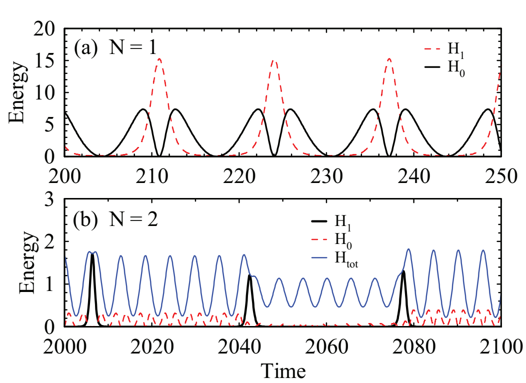

FIG. 3. (Color online) Intermediate forcing $f = 1$: energy distributions for (a) $N = 1$, intervals ≈ 13, and (b) $N = 2$.

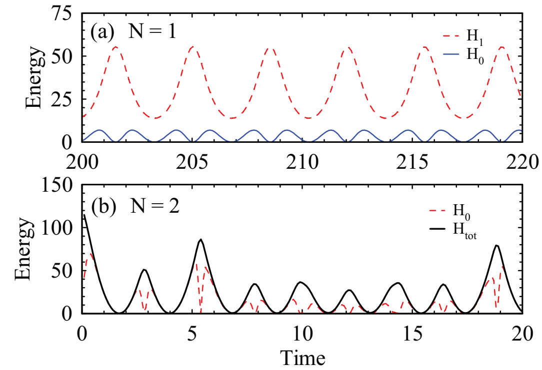

FIG. 4. (Color online) Strong forcing $f = 10$: energy distributions for (a) $N = 1$, intervals ≈ 3, and (b) $N = 2$.

This corresponds to a rescaling of the $H_0 - H_1$ cycle (23) by $\tilde{t} = 2t$ for time and $\tilde{b}_0 = 2b_0$, etc., for the amplitudes, and hence the energies quadruple.

(ii) For intermediate forcing with $f = 1$, the time scale between flow reversals decreases by an order of magnitude in the $N = 1$ truncation [see Fig. 3(a)]. Thus the intervals τ approach the duration of individual breathers. For the complete set of modes in $N = 2$ [Fig. 3(b)] the system is weakly nonlinear with a mixing of frequencies, $\omega/2, \omega, 3\omega/2$, and 2ω, where $\omega = 2\pi/\tau$ is defined by the interarrival times of the flow reversals [11]. The lowest frequency determines the amplitude modulation.

(iii) For strong forcing, $f = 10$, the flow reversals in the $N = 1$ truncation are regular [Fig. 4(a)], with intervals decreased by an order of magnitude relative to $f = 1$. The dominant part of energy is accumulated in waves. In the $N = 2$ truncation the dynamics become intermittent as in the regime behavior detected by Lorenz [9] in the discrete equations (1). The events lose their identities and the system becomes strongly nonlinear. A positive largest Lyapunov exponent (estimated by error growth) indicates that the system is chaotic.

These experiments reveal a vanishing long-term means of mean flow and wave-number amplitudes; hence the Liouville theorem (21) appears to be satisfied in the mean. For $N = 1$ this is based on the symmetry of the constant of motion H_f.

V. CONCLUSIONS

In summary, a continuous dynamical equation derived from the Lorenz-96 model is able to mimic several types of complex processes observed in geophysics, geophysical fluid dynamics, and solid-state physics:

(i) Avalanche processes excited by continuous driving as in the sandpile model of Bak *et al.* [12]; see also the recent observation of quasiperiodic events in crystal plasticity subject to external stress [13]. A common characteristic property is the weakness of the external forcing which is necessary to cause avalanches. In the present model the flow is driven by a constant forcing towards a state where mean flow and wave energy interact. The intervals between the flow reversals are approximately proportional to the inverse of the forcing intensity, $\sim 1/f$.

(ii) The quasibiennial oscillation (QBO, [14]), a flow reversal in the tropical stratosphere driven by two different types of upward-propagating gravity waves. A common aspect is that the driving of the mean flow by waves occurs only for a particular sign of the mean flow. Although the QBO is considered to be explained dynamically, the simulation in present-day weather and climate models necessitates careful subscale parametrizations or high-resolution models [15]. The present model is clearly an oversimplification but can be considered as a toy model for this phenomenon.

(iii) Rogue waves (also termed freak or monster waves) at the ocean surface are simulated mainly by the nonlinear Schrödinger equation (e.g., [16,17]); a Lagrangian analysis has been published recently [18]. The breather solutions found in the present model show characteristics such as the rapid evolution and the high intensity in an almost quiescent medium.

In the $N = 1$ truncation, a constant of motion for finite forcings can be derived (see H_f (22)) which reduces to the total energy for vanishing forcing. Initial conditions with a pronounced avalanche behavior can be identified as a regime with weak temporary wave intensity.

Due to the flow reversals, the total energy of the nondissipative system remains finite for a constant forcing. The long-term mean of the mean flow vanishes and the Liouville theorem (21) is satisfied in the mean. The flow reversals are insensitive to viscous dissipation.

ACKNOWLEDGMENTS

J.W. and V.L. acknowledge support from the European Research Council under the European Community's Seventh Framework Programme (FP7/2007-2013)/ERC Grant Agreement No. 257106. We would also like to thank the Cluster of Excellence CliSAP at the University of Hamburg.

APPENDIX: ALGEBRAIC DERIVATION

For $\gamma = F = 0$ the equations (1) are conservative with the conservation law, $H_X = 1/2 \sum_i X_i^2$, denoted as energy in the following. The dynamics in the state space of the X_i is nondivergent, thus satisfying Liouville's theorem, $\sum_i \partial \dot{X}_i / \partial X_i = 0$.

The dynamics of an observable function $Q(X)$ is given by

$$Q_t = \{Q, H_X\}, \tag{A1}$$

with the antisymmetric bracket

$$\{A,B\} = \partial_i A J_{ij} \partial_j B = -\{B,A\}, \tag{A2}$$

where $\partial_i = \partial/\partial X_i$, and the antisymmetric matrix

$$J_{ij} = X_{i-1}\delta_{j,i+1} - X_{j-1}\delta_{i,j+1}. \tag{A3}$$

Energy H_X is conserved due to the antisymmetry of the bracket.

The conservative terms of the Lorenz-96 equations (1) are obtained for $Q = X_i$. The equations are non-Hamiltonian [19] since the Jacobi identity

$$\sum_\ell J_{i\ell}\frac{\partial J_{jk}}{\partial X_\ell} + \sum_\ell J_{j\ell}\frac{\partial J_{ki}}{\partial X_\ell} + \sum_\ell J_{k\ell}\frac{\partial J_{ij}}{\partial X_\ell} = 0 \tag{A4}$$

is not satisfied.

We use the infinitesimal shift operators

$$L_\pm = \sum_{k=0}^{\infty} \frac{(\pm h \partial_x)^k}{k!} \tag{A5}$$

to write the bracket (A2) as

$$\{A,B\} = \int \frac{\delta A}{\delta u} \mathcal{J}_\infty \frac{\delta B}{\delta u} \tag{A6}$$

with

$$\mathcal{J}_\infty = (L_- u) \circ L_+ - L_- \circ (L_- u), \tag{A7}$$

where $(L_- u)$ is a multiplication operator. The bracket is antisymmetric since the adjoint is $L_+^* = L_-$.

By taking nth-order truncations of the operators $L_\pm$, we can find a hierarchy of truncated antisymmetric operators

$$\mathcal{J}_{nm} = (L_{-,n} u) \circ L_{+,m} - L_{-,m} \circ (L_{-,n} u), \tag{A8}$$

where

$$L_{\pm,n} = \sum_{k=0}^{n} \frac{(\pm h \partial_x)^k}{k!}. \tag{A9}$$

To each of these truncated operators corresponds a continuous Lorenz-96 model

$$u_t = \{u, \mathcal{H}\}_{nm}, \tag{A10}$$

where the indices indicate the operator $\mathcal{J}_{nm}$. [As in Eq. (1), periodic boundary conditions are assumed.]

[1] E. N. Lorenz, *Proc. Seminar on Predictability, ECMWF*, Vol. 1 (Reading, Berkshire, 1996), pp. 1–18.
[2] R. Abramov and A. J. Majda, Nonlinearity **20**, 2793 (2007).
[3] S. Hallerberg, D. Pazo, J. M. Lopez, and M. A. Rodriguez, Phys. Rev. E **81**, 066204 (2010).
[4] V. Lucarini, J. Stat. Phys. **146**, 774 (2012).
[5] V. Lucarini and S. Sarno, Nonlin. Processes Geophys. **18**, 728 (2011).
[6] J. T. Ambadan and Y. Tang, J. Atmos. Sci. **66**, 261 (2009).
[7] S. Khare and L. A. Smith, Mon. Weather Rev. **139**, 2080 (2011).
[8] J. W. Messner and G. J. Mayr, Mon. Weather Rev. **139**, 1960 (2011).
[9] E. Lorenz, J. Atmos. Sci. **63**, 2056 (2006).
[10] E. Lorenz, J. Atmos. Sci. **62**, 1574 (2005).
[11] V. Lucarini and K. Fraedrich, Phys. Rev. E **80**, 026313 (2009).
[12] P. Bak, C. Tang, and K. Wiesenfeld, Phys. Rev. Lett. **59**, 381 (1987).
[13] S. Papanikolaou, D. M. Dimiduk, W. Choi, J. P. Sethna, M. D. Uchic, C. F. Woodward, and S. Zapperi, Nature (London) **490**, 517 (2012).

[14] M. P. Baldwin, L. J. Gray, T. J. Dunkerton, K. Hamilton, P. H. Hayne, W. J. Randel, J. R. Holton, M. J. Alexander, I. Hirota, T. Horinouchi, D. B. A. Jones, J. S. Kinnersley, C. Marquardt, K. Sato, and M. Takahasi, Rev. Geophys. **39**, 179 (2001).

[15] Y. Kawatani, K. Sato, T. J. Dunkerton, S. Watanabe, S. Miyahara, and M. Takahashi, J. Atmos. Sci. **67**, 963 (2010).

[16] M. Onorato, A. R. Osborne, and M. Serio, Phys. Rev. Lett. **96**, 014503 (2006).

[17] A. Calini and C. M. Schober, Nonlinearity **25**, R99 (2012).

[18] A. Abrashkin and A. Soloviev, Phys. Rev. Lett. **110**, 014501 (2013).

[19] A. Sergi and M. Ferrario, Phys. Rev. E **64**, 056125 (2001).